The 8th European Congress on Computational Methods in Applied Sciences and Engineering
ECCOMAS Congress 2022
5-–9 June 2022, Oslo, Norway

THE STARRY NIGHT OF REACTION DIFFUSION, WINNER OF THE ARTS & SCIENCE CONTEST

Fleurianne Bertrand[1]

[1]Faculty of Electrical Engineering, Mathematics and Computer Science, University of Twente
f.bertrand@utwente.nl

Key words: Computational Mechanics, FEM, Contact Problems

Abstract. The Arts and Science Contest of the ECCOMAS Young Investigators Committee (EYIC) aims to show science in all its beauty and elegance, by visualizing scientific works with an artistic point of view. The competition was open to every participant with an accepted abstract, the visuals were uploaded in 4 groups on the ECCOMAS Facebook page, one group per week. The visual with the most likes of each group was put in the finalists short-list, and a jury chose the final winners of the contest. *The starry night of reaction diffusion* won this competition and the present contribution presents the numerical method behind the picture.

Figure 1: The starry night of reaction diffusion

1 The Gray-Scott equations

On a domain $\Omega \subset \mathbb{R}^d$ and a time interval $I = [0, t_N]$, let $u : \Omega \times I$ describe a density of a physical quantity (concentration of a substance, population density, temperature, ...). In the absence of external forces, a diffusion process takes place, i.e. there is a movement from a region of higher concentration to a region of lower concentration. This physical process is usually modelled by the following partial differential equation:

$$\frac{\partial u}{\partial t} = \alpha \Delta u \tag{1}$$

where α is the diffusion coefficient. Let us now consider a second density $v : \Omega \times I$. The diffusion and reaction between the two quantities is given by the coupled system

$$\begin{aligned} \frac{\partial u}{\partial t} &= \alpha_u \Delta u + f_u(u, v) \\ \frac{\partial v}{\partial t} &= \alpha_v \Delta v + f_v(u, v) \ , \end{aligned} \tag{2}$$

where the functions $f_u(u, v)$ and $f_v(u, v)$ are the local reaction rates. The Gray-Scott problem originally describes (see [14]) two chemical reactions such that the reaction rates are given by

$$f_u(u, v) = -uv^2 + \beta(1 - u) \text{ and } f_v(u, v) = -uv^2 - (\beta + \gamma) \tag{3}$$

where β and γ are two parameters called feed rate and kill rate, see also [15]. This model presents self-replicating patterns occuring in natural phenomenons such as spots and strips. It is also used to describe patterns in biomedical applications, see [13].

2 Spatial finite difference scheme

The numerical scheme for the discretisation of System (2) is a finite difference scheme, i.e. the derivatives are replaced by differential quotients. The spatial domain Ω is discretised with an equidistant grid with mesh size h.

A first way to obtain a spatial finite difference scheme is the simple second-order central scheme in each dimension:

$$\frac{\partial^2 u}{\partial x^2}(x, y) \approx \frac{\frac{u(x+h,y)-u(x,y)}{h} - \frac{u(x,y)-u(x-h,y)}{h}}{h} = \frac{u(x + h, y) - 2u(x, y) + u(x - h, y)}{h^2}, \tag{4}$$

$$\frac{\partial^2 u}{\partial y^2}(x, y) \approx \frac{\frac{u(x,y+h)-u(x,y)}{h} - \frac{u(x,y)-u(x,y-h)}{h}}{h} = \frac{u(x, y + h) - 2u(x, y) + u(x, y - h)}{h^2} \ . \tag{5}$$

The corresponding approximation of the two-dimensional Laplacian therefore uses the five point stencil $\{(x - h, y), (x, y), (x + h, y), (x, y - h), (x, y + h)\}$ of a point (x, y):

$$\Delta u(x, y) \approx \frac{1}{h^2} \left(u(x + h, y) + u(x - h, y) + u(x, y + h) + u(x, y - h) - 4u(x, y) \right). \tag{6}$$

The error in this approximation is $O\left(h^2\right)$. In the presence of periodic boundary conditions, the matlab function Y = circshift(X,k,d) can be used as it circularly shifts the elements in the array X by k positions along the dimension d. This gives rise to the following matlab function that computes the approximation of the laplacian of a discrete field U.

Algorithm 1: 5-points finite difference

```
function LU = laplacian(U)
LU = -U;
for d = 1:2
    for j=-1:2:1
        LU = LU + 0.25*circshift(U,j,d);
    end
end
end
```

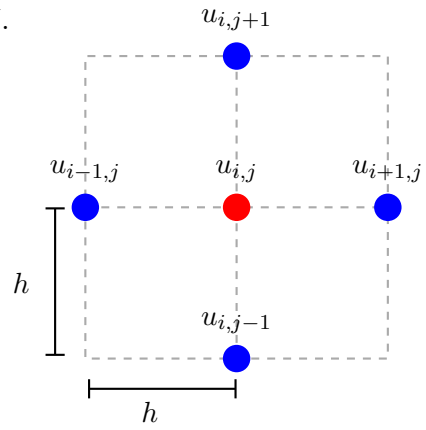

Figure 2: 5-points scheme

3 Discretisation of the Gray-Scott equation

For the discretisation in time of the Gray-Scott equation, the interval I is divided into n non overlapping intervals $[t_k, t_{k+1}]$, $k = 0, 1, .., n$ of the same length $t_{k+1} - t_k = t_1$. The time derivative is then approximated by an explicit forward differential quotient

$$\frac{\partial u}{\partial t}(t + t_1, x, y) \approx \frac{u(t + t_1, x, y) - u(t, x, y)}{t_1} \ . \tag{7}$$

Let $U_{k,i,j}$ and $V_{k,i,j}$ denote the discrete approximations of u and v at the point $(t_k, ih, jh) \in I \times \Omega$. Inserting the time discretisation scheme (7) into the Gray-Scott equations (2) leads to the numerical scheme

$$\begin{aligned} U_{k+1,i,j} &= U_{k,i,j} + t_1 \left(\alpha_u LU_{k,i,j} + f_u(U_{k,i,j}, V_{k,i,j})\right) \\ V_{k+1,i,j} &= V_{k,i,j} + t_1 \left(\alpha_v LV_{k,i,j} + f_v(U_{k,i,j}, V_{k,i,j})\right) \ , \end{aligned} \tag{8}$$

where $LU_{k,i,j}$ (respectively $LV_{k,i,j}$) is an approximation of Δu (respectively Δv) at the point $(t_k, ih, jh) \in I \times \Omega$. This leads to the following algorithm.

Algorithm 2: Gray-Scott algorithm

```
function [U,V]=GrayScott(U0,V0,n,alu,alv,beta,gamma,dt,s)
U=U0; V=V0;
for i = 1:n
    fu = -U.*V.^2+beta.*(1.-U); fv = +U.*V.^2-(beta+gamma).*V;
    U = U+dt*(alu.*(laplacian(U,s))+fu);
    V = V+dt*(alv.*(laplacian(V,s))+fv);
end
end
```

4 Pattern formation

The Gray-Scott system is known to be able to describe patterns that occur in nature, especially due to the work of Alan Turing in [16] who discovered in particular that a stable stationary state becomes unstable when a diffusive phenomenon occurs. The relation between the parameters $\alpha_u, \alpha_v, \beta$ and γ is therefore crucial. For $c \in \mathbb{R}$, let $\mathbb{C}_c^{d_1 \times d_2} \in \mathbb{R}^{d \times d}$ denote the matrix with $\left(\mathbb{C}_c^{d_1 \times d_2}\right)_{ij} = c$ for all $1 \leq i \leq d_1$ and $1 \leq j \leq d_2$. The initial conditions for this first example are given by $u_0, v_0 \in \mathbb{R}^{400 \times 400}$ such that

$$u_0 = \begin{pmatrix} & \mathbb{C}_1^{194\times 400} & \\ \left(\mathbb{C}_1^{11\times 194}\right. & \mathbb{C}_0^{11\times 11} & \left.\mathbb{C}_1^{11\times 195}\right) \\ & \mathbb{C}_1^{195\times 400} & \end{pmatrix} \quad v_0 = 1 - u_0.$$

For $\beta = 0.02 + 0.01k$ and $\gamma = 0.045 + 0.001l$, $k, l \in \{0, ..., 20\}$ we gather the different patterns in Figure 3.

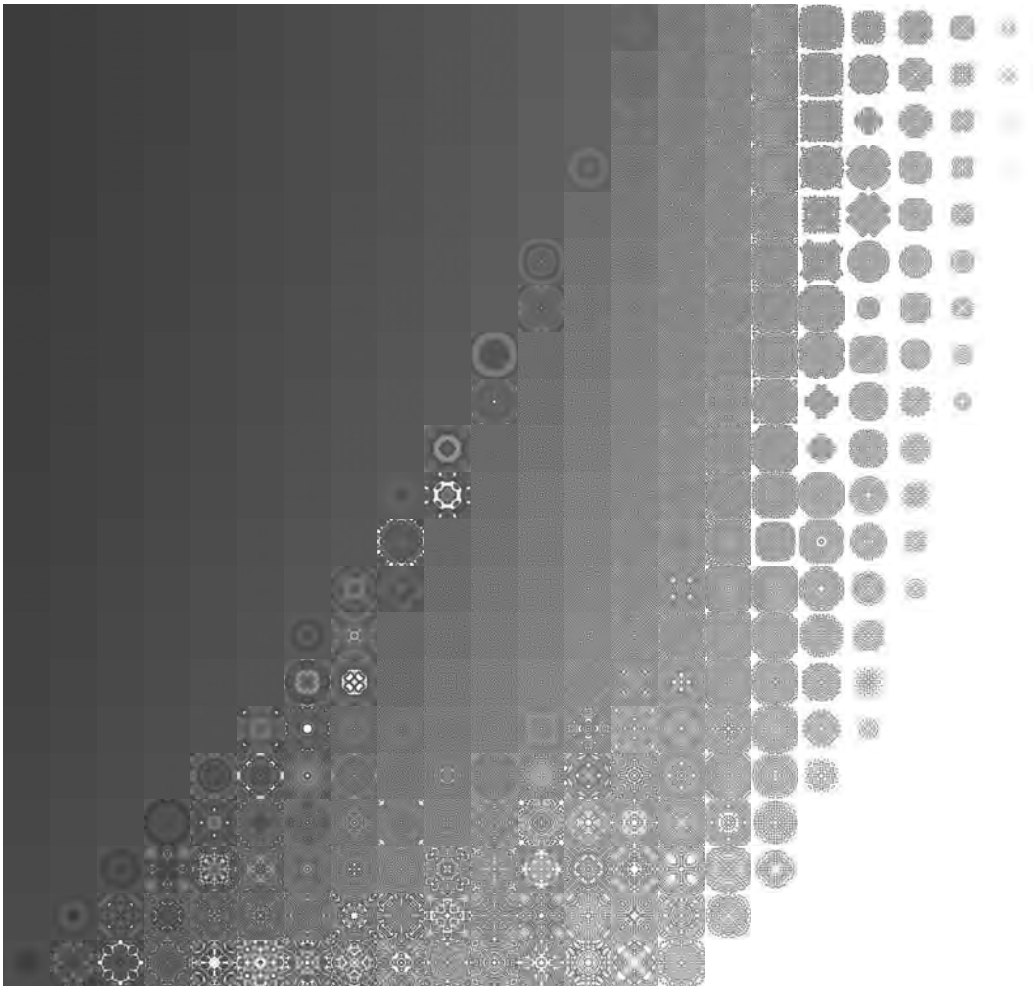

Figure 3: Different patterns obtained for $\beta = 0.02{+}0.01k$ and $\gamma = 0.045{+}0.001l$, $k, l \in \{0, ..., 20\}$.

A detailed view of the diagonal elements is show in the following Figure 4.

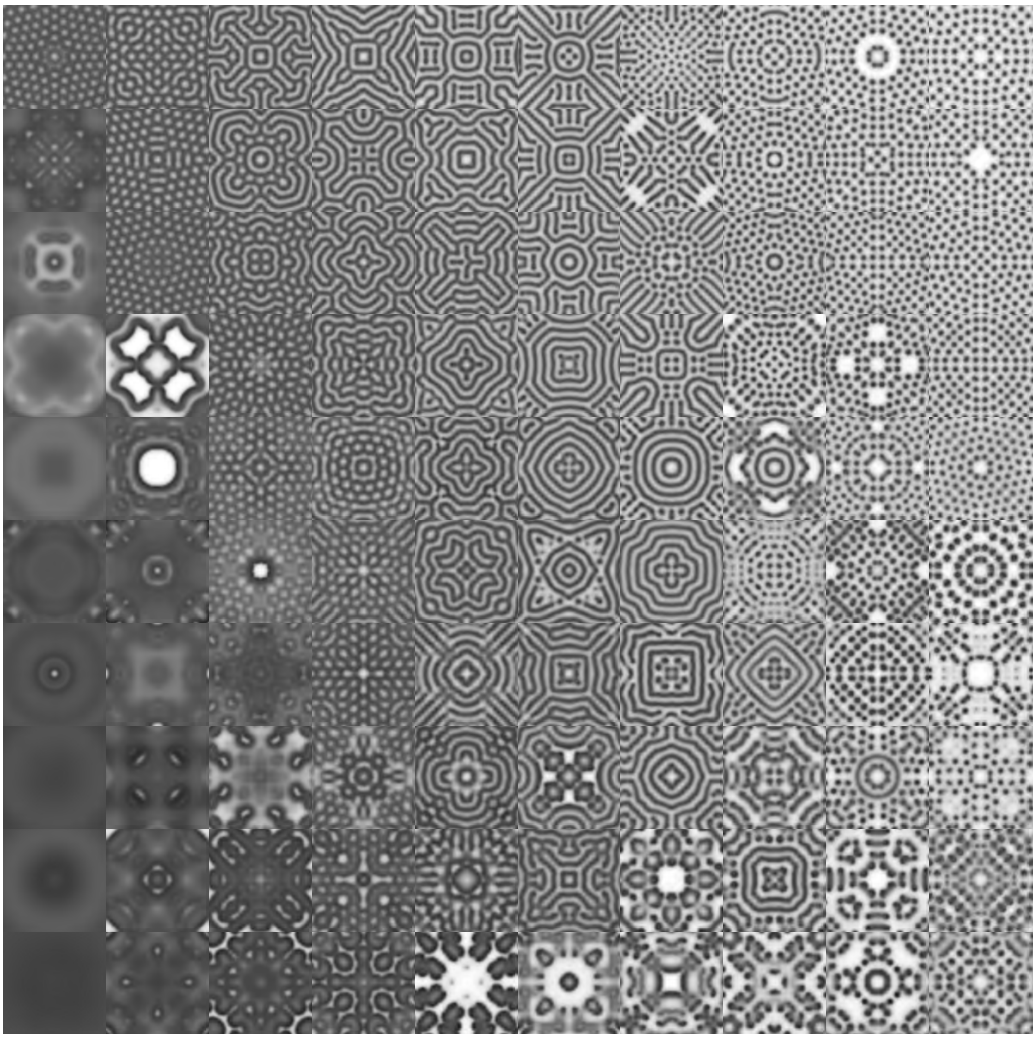

Figure 4: Different patterns obtained for $\beta = 0.02{+}0.01k$ and $\gamma = 0.045{+}0.001l$, $k, l \in \{0, ..., 20\}$.

5 Further numerical examples

This section states the parameters and initial conditions leading to the elements of the picture of Figure 1. The initial conditions to obtain the stars of Figure 1 are similar to the initial conditions of the example of the previous section: $u_0, v_0 \in \mathbb{R}^{100\times 100}$ such that

$$u_0 = \begin{pmatrix} & \mathbb{C}_1^{45\times 100} & \\ (\mathbb{C}_1^{10\times 45} & \mathbb{C}_0^{10\times 10} & \mathbb{C}_1^{10\times 45}\ ) \\ & \mathbb{C}_1^{45\times 100} & \end{pmatrix}, \quad v_0 = 1 - u_0.$$

Using $\alpha_u = 1$, $\alpha_u = 0.5$, $\beta = 0.04$ and $\gamma = 0.0636$, we obtain the stars of the Figure 1.

Figure 5: Approximation of u at time step t=0,280,520,780,1040,1300,1560,1820

5.1 Waves

To obtain the wave pattern of Figure 1, we consider the matrix $\bar{u} = (1,1,1)^\top \left(\frac{3}{4}, \frac{1}{2}, \frac{1}{4}, 0\right)$ and $\bar{u}_0 = \bar{u}(:)\mathbb{C}_1^{1\times 61} \in \mathbb{R}^{12\times 61}$. We now set

$$u_0 = \begin{pmatrix} & \mathbb{C}_1^{394\times 800} & \\ (\mathbb{C}_1^{12\times 370} & \bar{u}_0 & \mathbb{C}_1^{12\times 269} \quad) \\ & \mathbb{C}_1^{394\times 800} & \end{pmatrix}, \quad \text{and} \quad v_0 = \begin{pmatrix} & \mathbb{C}_1^{394\times 800} & \\ (\mathbb{C}_1^{12\times 370} & \mathbb{C}_0^{12\times 61} & \mathbb{C}_1^{12\times 269} \quad) \\ & \mathbb{C}_1^{394\times 800} & \end{pmatrix}.$$

Using $\alpha_u = 1$, $\alpha_u = 0.5$, $\beta = 0.04$ and $\gamma = 0.0636$, we obtain the waves of Figure 1.

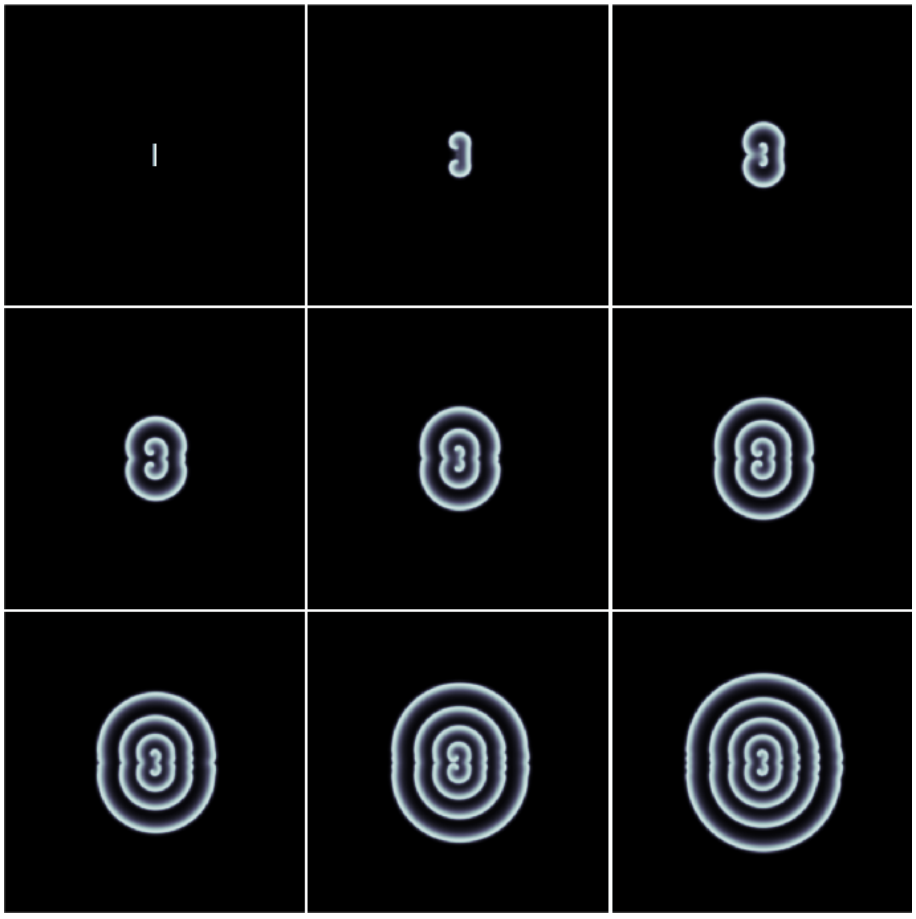

Figure 6: Approximation of u at time step t=0,300,...,2400

6 Effects of the finite difference scheme

In order to analyse the effect of the discretisation scheme, we now compare the results using a discretisation scheme with more points. A first possibility is to add the diagonal points, as shown in Figure 6. We first note that the square formed with the violet points $\{u_{i-1+k,j-1+l}\}$ for $k,l \in \{0,2\}$ is obtained from the square formed by the blue points $\{u_{i+k(2l-1),j+(2l-1)(1-k)}\}$ for $k,l \in \{0,1\}$ by rotating by $\frac{\pi}{2}$ and scaling by $\sqrt{2}$.

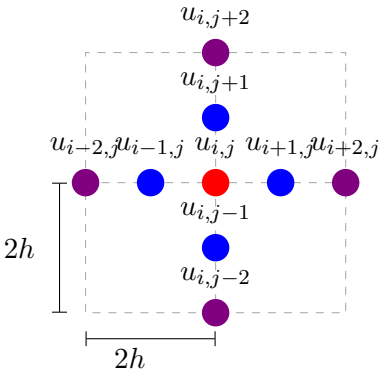

Figure 7: 9-points scheme

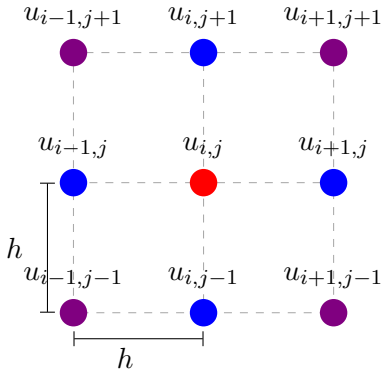

Figure 8: 9-points scheme with diagonal points

Rewriting Equation (6) accordingly leads to

$$\Delta u(x,y) \approx \frac{1}{2h^2}\left(u(x+h,y+h)+u(x-h,y-h)+u(x-h,y+h)+u(x+h,y-h)-4u(x,y)\right). \quad (9)$$

We can now weight the two schemes (6) and (9) with some $\delta_1, \delta_2 > 0$ to obtain:

$$\begin{aligned}\Delta u(x,y) &\approx \frac{\delta_1}{2h^2}\left(u(x+h,y+h)+u(x-h,y-h)+u(x-h,y+h)+u(x+h,y-h)-4u(x,y)\right)\\ &\quad+\frac{\delta_2}{h^2}\left(u(x+h,y)+u(x-h,y)+u(x,y+h)+u(x,y-h)-4u(x,y)\right),\\ \text{i.e. } \Delta u(x,y) &\approx -2\frac{\delta_1+2\delta_2}{h^2}u(x,y)+\frac{\delta_2}{h^2}\left(u(x+h,y)+u(x-h,y)+u(x,y+h)+u(x,y-h)\right)\\ &\quad+\frac{\delta_1}{2h^2}\left(u(x+h,y+h)+u(x-h,y-h)+u(x-h,y+h)+u(x+h,y-h)\right).\end{aligned} \quad (10)$$

A typical choice is $\delta_1 = 2$ and $\delta_2 = 4$, as chosen in the following algorithm.

Algorithm 3: 9-points finite difference

```
function LU = laplacian(U)
    LU = -U;
    for i=-1:2:1
        LU = LU+0.2*(circshift(U,i)+circshift(U,i,2));
        for j=-1:2:1
            LU = LU+0.05*circshift(U,[i j]);
        end
    end
end
```

Another possibility for the numerical scheme corresponding to the discretisation of the system (2) is to consider the nine points around the point $u_{i,j}$ instead of the five of Figure 2. For this, we consider the following Taylor expansions of u

$$u(x \pm h, y) \approx u(x,y) \pm h u_x(x,y) + \frac{h^2}{2} u_{xx}(x,y) \pm \frac{h^3}{6} u_{xxx}(x,y) + \frac{h^4}{24} u_{4x}(x,y) \pm \frac{h^5}{120} u_{5x}(x,y)$$
$$u(x \pm 2h, y) \approx u(x,y) \pm 2h u_x(x,y) + 2h^2 u_{xx}(x,y) \pm \frac{4}{3} h^3 u_{xxx}(x,y) + \frac{2}{3} h^4 u_{4x}(x,y) \pm \frac{32}{120} h^5 u_{5x}(x,y) \ .$$

Combining the above equations leads to

$$u(x+h,y) + u(x-h,y) = 2u(x,y) + h^2 u_{xx}(x,y) + \frac{h^4}{12} u_{4x}(x,y)$$
$$u(x+2h,y) + u(x-2h,y) = 2u(x,y) + 4h^2 u_{xx}(x,y) + \frac{4}{3} h^4 u_{4x}(x,y)$$

and thus to

$$u(x+h,y) + u(x-h,y) - \frac{1}{16}\left(u(x+2h,y) + u(x-2h,y)\right) \approx \frac{15}{8} u(x,y) + \frac{3}{4} h^2 u_{xx}(x,y) \ ,$$

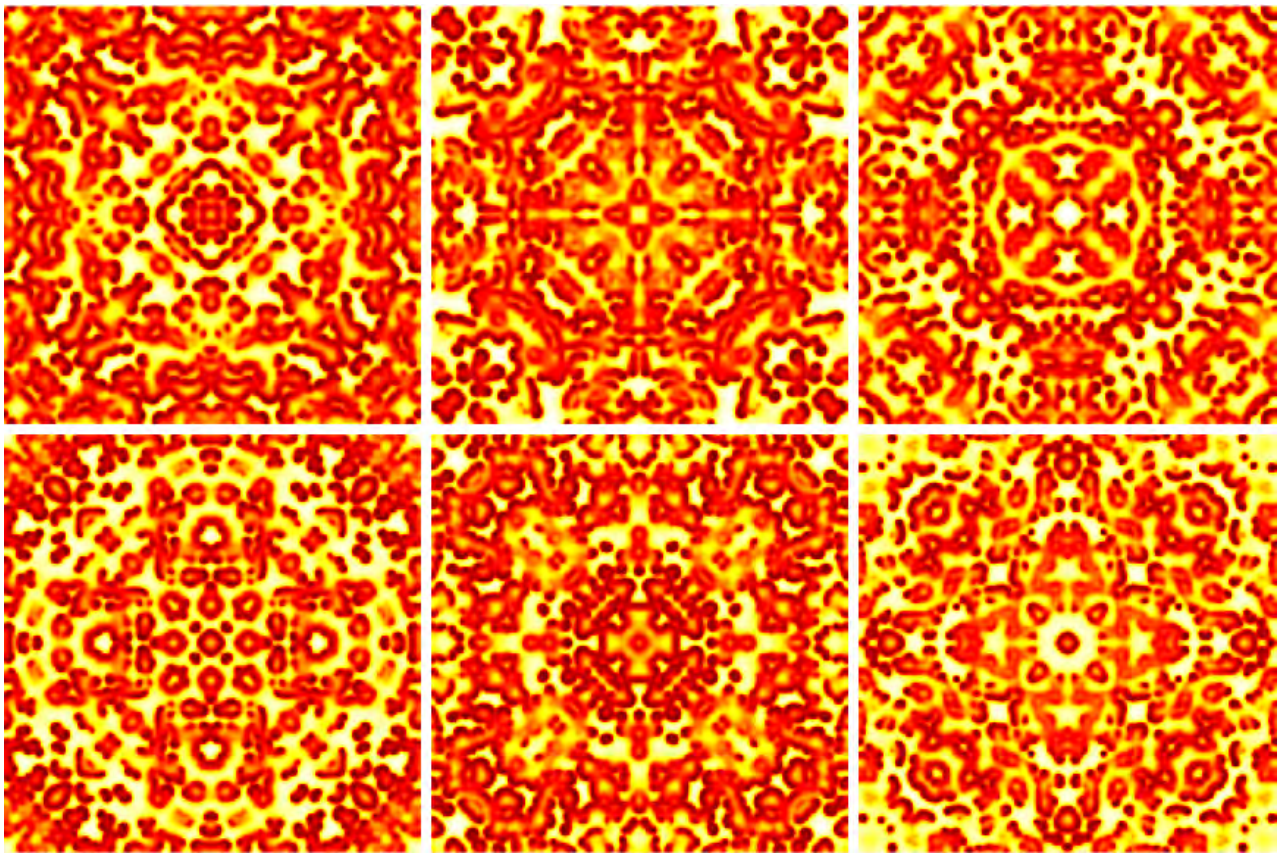

Figure 9: Effects of the diagonal points in finite difference scheme. Top left: nine point scheme (10) with $\delta_1 = 2$ and $\delta_2 = 4$. Bottom right $\delta_1 = 0$ and $\delta_2 = 1$. From top left to bottom right with $\delta_1 = \{2, 1.6, 1.2, 0.8, 0.4, 0\}$ and $\delta_2 = 1.5\delta_1$.

i.e.

$$u_{xx} \approx \frac{1}{2h^2}\left(\frac{2}{3}u(x+h,y)+\frac{2}{3}u(x-h,y)-\frac{1}{6}u(x+2h,y)-\frac{1}{6}u(x-2h,y)-5u(x,y)\right) . \quad (11)$$

Performing the same Taylor expansions in the y direction, we obtain the following approximation

$$u_{yy} \approx \frac{1}{2h^2}\left(\frac{2}{3}u(x,y+h)+\frac{2}{3}u(x,y-h)-\frac{1}{6}u(x,y+2h)-\frac{1}{6}u(x,y-2h)-5u(x,y)\right) . \quad (12)$$

Combining (11) and (12), we obtain the following discretisation scheme

$$\begin{aligned}\Delta u(x,y) \approx \frac{1}{3h^2}\Big(&\frac{2}{3}u(x+h,y)+\frac{2}{3}u(x-h,y)-\frac{1}{6}u(x+2h,y)-\frac{1}{6}u(x-2h,y)\\ &\frac{2}{3}u(x,y+h)+\frac{2}{3}u(x,y-h)-\frac{1}{6}u(x,y+2h)-\frac{1}{6}u(x,y-2h)-10u(x,y)\Big) .\end{aligned}$$

Some effects of the different finite difference scheme are shown in Figure 9.

7 INTERPLAY WITH RESEARCH FIELD

One of the recurrent question during the presentation of this picture is how it relates to my research field. Surely, the effects mentioned in the previous section are not negligible and further numerical schemes will be considered in future works. In particular, finite element methods can be considered. A particular application of interest is the formation of pattern in elastic or porous solids. In those applications, the computation of the dual variable is crucial, see [10, 11]. Note that for application involving domain with curved boundaries, parametric $H(div)$ discretisation spaces as in [1, 8, 9] are required. In order to combine the accuracy of its approximation with an inherent adaptive error estimator, Least-Squares and dPG methods are promising, see [4]. As an alternative, fluxes and stresses can be reconstruct from the primal approach and the difference between them can be used as an error estimator ([5, 7, 2, 3, 6]).

8 ACKNOWLEDGEMENTS

I would like to thank the Young Investigator committee of the Eccomas for organising this competition, motivating me to reactivate the corresponding mandatory social account to be able to participate. Even though navigating between the personal and professional posts was not easy, the kind words about my work warmed my heart day after day.

I am beyond grateful to all the account owners that liked and voted for my picture, especially the ones who created an account to support me. I am also extremely thankful to my family and my friends for disseminating my contribution with warm encouragements. This award is yours, as I could not have done it without you.

REFERENCES

[1] F. Bertrand. First-order system least-squares for interface problems. *SIAM Journal on Numerical Analysis*, 56(3):1711–1730, 2018.

[2] F. Bertrand and D. Boffi. The Prager–Synge theorem in reconstruction based a posteriori error estimation. In *75 years of mathematics of computation*, volume 754 of *Contemp. Math.*, pages 45–67. Amer. Math. Soc., Providence, RI, 2020.

[3] F. Bertrand, D. Boffi, and S. Stenberg. Asymptotically exact a posteriori error analysis for the mixed laplace eigenvalue problem. *Computational Methods in Applied Mathematics*, 20(2):215–225, 2020.

[4] F. Bertrand, Z. Cai, and Eun Y. Park. Least-squares methods for elasticity and Stokes equations with weakly imposed symmetry. *Computational Methods in Applied Mathematics*, 19(3):415–430, 2019.

[5] F. Bertrand, L. Demkowicz, and J. Gopalakrishnan. Recent advances in least-squares and discontinuous petrov–galerkin finite element methods. *Computers and Mathematics with Applications*, 95:1–3, 2021.

[6] F. Bertrand, B. Kober, M. Moldenhauer, and G. Starke. Weakly symmetric stress equilibration and a posteriori error estimation for linear elasticity. *Numerical Methods for Partial Differential Equations*, 37(4):2783–2802, 2021.

[7] F. Bertrand, M. Moldenhauer, and G. Starke. A posteriori error estimation for planar linear elasticity by stress reconstruction. *Computational Methods in Applied Mathematics*, 19(3):663–679, 2019.

[8] F. Bertrand, M. Moldenhauer, and G. Starke. Stress equilibration for hyperelastic models. *Lecture Notes in Applied and Computational Mechanics*, 98:91–105, 2022.

[9] F. Bertrand, S. Münzenmaier, and G. Starke. First-order system least squares on curved boundaries: higher-order Raviart-Thomas elements. *SIAM Journal on Numerical Analysis*, 52(6):3165–3180, 2014.

[10] F. Bertrand, S. Münzenmaier, and G. Starke. First-order system least squares on curved boundaries: lowest-order Raviart-Thomas elements. *SIAM Journal on Numerical Analysis*, 52(2):880–894, 2014.

[11] F. Bertrand and G. Starke. A posteriori error estimates by weakly symmetric stress reconstruction for the biot problem. *Computers and Mathematics with Applications*, 91:3–16, 2021.

[12] V. Cristini and J. Lowengrub. *Multiscale modeling of cancer: An integrated experimental and mathematical modeling approach*, volume 9780521884426. 2010.

[13] P. Gray and S.K. Scott. Autocatalytic reactions in the isothermal, continuous stirred tank reactor. oscillations and instabilities in the system a + 2b $\rightarrow$ 3b; b $\rightarrow$ c. *Chemical Engineering Science*, 39(6):1087–1097, 1984.

[14] K.J. Lee, W.D. McCormick, Q. Ouyang, and H.L. Swinney. Pattern formation by interacting chemical fronts. *Science*, 261(5118):192–194, 1993.

[15] A.M. Turing. The chemical basis of morphogenesis. *Bull Math Biol.*, 52(1):53–97, 1990.